Free Radical Research, June 2009; 43(6): 581–593

Electron transfer: A primary step in the reactions of sodium hydrosulphide, an H_2S/HS^- donor

ANDREJ STAŠKO[1], VLASTA BREZOVÁ[1], MICHAL ZALIBERA[1], STANISLAV BISKUPIČ[1], & KAROL ONDRIAŠ[2]

[1]*Institute of Physical Chemistry and Chemical Physics, Faculty of Chemical and Food Technology, Slovak University of Technology in Bratislava, Radlinského 9, SK-812 37 Bratislava, Slovak Republic, and* [2]*Institute of Molecular Physiology and Genetics, Centre of Excellence for Cardiovascular Research, Slovak Academy of Sciences, Vlárska 5, SK-833 34 Bratislava, Slovak Republic*

(Received 5 March 2009; revised 7 April 2009)

Abstract
Endogenously produced H_2S/HS^-, a newly found gasotransmitter, is well represented by NaHS. In deoxygenated media it terminated semi-stable oxidant radicals up to stoichiometric ratios of 1:1. In the presence of oxygen the antioxidant activities of NaHS were impaired considerably due to its competitive reactions with molecular oxygen. The primary reaction steps of NaHS were investigated using two different spin traps, 5,5-dimethylpyrroline-N-oxide and sodium 3,5-dibromo-4-nitrosobenzenesulphonate (DBNBS), in protolytic and aprotic solvents (water and dimethylsulphoxide, DMSO) under argon and oxygen. Sulphhydryl radicals ($HS^\bullet/S^{\bullet-}$) were primarily formed ($S^{\bullet-}$ in water and $HS^\bullet$ in DMSO), probably coupled to the formation of superoxide radical anions. The DBNBS spin trap acted also as an electron acceptor and formed its radical anions in the presence of NaHS. Hence, one of the primary steps in the reactions of sulphides is the electron transfer from H_2S/HS^- species to a suitable acceptor, which may play a fundamental role in their biological functions.

Keywords: *Sodium hydrosulphide, hydrogen sulphide, antioxidant, electron transfer, donor, sulphhydryl radical, spin traps*

Abbreviations: *DPPH, 1,1-diphenyl-2-picrylhydrazyl; ABTS, 2,2′-azinobis-(3-ethylbenzothiazoline-6-sulphonate); DMPO, 5,5-dimethylpyrroline-N-oxide; DBNBS, sodium 3,5-dibromo-4-nitrosobenzenesulphonate; DMSO, dimethyl sulphoxide; SW, magnetic field sweep width; TEMPOL, 4-hydroxy-2,2,6,6-tetramethylpiperidine N-oxyl*

Introduction

Endogenously produced H_2S in living organism is a newly-found gasotransmitter influencing numerous biological processes in which free radicals were supposed to play a significant role. It is involved in cardioprotection, hypertension, relaxation, proliferation, apoptosis and inflammation processes [1–8]. The role of H_2S in the regulation of nitric oxide was evidenced previously [9–14].

Several reports suggested that H_2S/HS^- could function as an antioxidant. This suggestion was supported by the observation that H_2S was produced by oxidative stress [15] and protected neurons from oxidative stress, probably by scavenging free radicals [16]. Because H_2S/HS^- is a reducing agent that readily reacts with hydrogen peroxide [17,18], it was assumed that an endogenous H_2S/HS^- could scavenge oxygen species [19–22], peroxynitrite [23–26] and hypochlorite [27,28]. In the presence of molecular oxygen and trace metal catalysts, sulphides were spontaneously oxidized. Oxidation-reduction reactions frequently involve free-radical intermediates

Correspondence: Professor Andrej Staško, Institute of Physical Chemistry and Chemical Physics, Faculty of Chemical and Food Technology, Slovak University of Technology in Bratislava, Radlinského 9, SK-812 37 Bratislava, Slovak Republic. Tel: +421 2 59325 475. Fax: +421 2 52926 032. Email: andrej.stasko@stuba.sk

ISSN 1071-5762 print/ISSN 1029-2470 online
DOI: 10.1080/10715760902977416

and a metal-catalysed pathway has been proposed [29], in which the initial reactions of sulphide oxidation form superoxide and sulphide radicals. The production of oxygen- and sulphur-centred free radicals was also proposed during the oxidation of sulphide in seawater [30]. However, the antioxidant properties and radical reactions of sulphidic systems are not fully understood. Therefore in our work we investigated scavenging activities and radical mechanisms of NaHS action donating $HS^{\bullet}/S^{\bullet-}$ species.

Referring to H_2S, NaHS is recommended as its suitable donor [31]. Assuming we work with initial NaHS concentration, c_0, in neutral aqueous solutions ($pH = 7$, $c_{OH} = c_H \cong 1 \times 10^{-7}$ mol/dm^3, activities a_{H^+,OH^-} approximated with concentrations c_{H^+,OH^-}), a complete dissociation of NaHS to Na^+ and HS^- is expected ($NaHS \leftrightarrow Na^+ + HS^-$) and the second-stage dissociation to S^{2-} is negligible ($HS^- \leftrightarrow H^+ + S^{2-}$; $K_{2,H_2S} = 1 \times 10^{-19}$ at 25°C [32]); consequently the concentration of S^{2-} can be neglected. What is decisive for the concentration of H_2S is the hydrolysis of HS^- [33], namely, $HS^- + H_2O \leftrightarrow H_2S + OH^-$, described by the hydrolysis constant $K_{HS^-} = \frac{K_w}{K_{1,H_2S}} = 1.13 \times 10^{-7}$, where $K_w = 1.008 \times 10^{-14}$ is the ionic product of water (25°C) and $K_{1,H_2S} = 8.91 \times 10^{-8}$ is the first-stage dissociation constant of H_2S at 25°C [32].

$$K_{HS^-} = \frac{c_{H_2S} c_{OH^-}}{c_{HS^-}} = 1.13 \times 10^{-7} \qquad (1)$$

In buffer solutions at $pH = 7$ the initial concentration of NaHS, c_0, is practically totally converted to two species, HS^- and H_2S (S^{2-} is neglected); hence $c_0 = c_{HS^-} + c_{H_2S}$. Inserting the presented data in the hydrolysis constant K_{HS^-} (equation 1) it turns out that, approximately, $c_{H_2S} \cong c_{HS^-} \cong 0.5c_0$. This means that, in neutral aqueous solutions, 50% of NaHS is converted to H_2S; consequently the ratio $\frac{c_{H_2S}}{c_{HS^-}} \cong 1$, and it is well justified to speak about an H_2S/HS^- system. It should be added that the H_2S concentration does change very sensitively with pH values [31].

Our investigations were focused on the primary reaction steps of NaHS under various conditions. First, using two different types of oxidant radicals (DPPH, $ABTS^{\bullet+}$), the antioxidant properties of NaHS were investigated, indicating here a dominant role of molecular oxygen. Thus, systematic investigations in aerobic and anaerobic conditions, using two different spin trapping agents (DMPO, DBNBS) in protolytic and aprotic solvents (H_2O, DMSO) were carried out, monitoring the reactions by electron paramagnetic resonance (EPR) spectroscopy.

Material and methods

Materials

Chemicals used originated from the following sources: ABTS, DBNBS, DMPO and NaHS from Sigma-Aldrich (St. Louis, MO); DPPH from Fluka (Buchs, Switzerland); $K_2S_2O_8$, DMSO from Merck (Darmstadt, Germany); deuterated water from the Research Center for Applied Nuclear Physics (Dubna, Russian Federation); ethanol of spectroscopic grade (Microchem, Pezinok, Slovak Republic). Spin trapping agent DMPO was vacuum distilled and stored at −18°C prior to use. Phosphate buffer was prepared according to Sörensen, mixing KH_2PO_4 and Na_2HPO_4 (Lachema, Brno, Czech Republic) solutions.

Preparation of solutions

Considering the lability of NaHS solutions (the tendency of H_2S to escape from the solution to air; the reaction of NaHS with oxygen) the corresponding solvents (H_2O or DMSO) were first saturated with argon, then solid NaHS was added, giving the required concentrations, and the argon bubbling was stopped. Generally, further manipulations with NaHS solution were carried out under argon. Spin trap solutions (DMPO, DBNBS) were prepared and used in air or in some experiments were also bubbled with argon or oxygen as specified below. Aqueous solutions of $ABTS^{\bullet+}$ were prepared as described in Re et al. [34]. DPPH was dissolved in ethanol, due to its low solubility in water [35].

EPR measurements

The EPR measurements were carried out in a flat cell (WG-812, Wilmad-LabGlass, USA) adapted for the flow-technique in a Bruker TM-110 (ER 4103 TM) cylindrical cavity using a Bruker EMX EPR spectrometer working in the X-band. Individual reactant solutions (DPPH, $ABTS^{\bullet+}$, spin trap or NaHS) were filled in separate syringes and simultaneously injected, via a small mixing chamber, into a flat cell placed in the cavity of the EPR spectrometer. The monitoring of EPR spectra started immediately after the injection. Various spectrometer settings (according to stability, time scale, required quality of recorded spectra) were used. The ER 4111 VT temperature unit (Bruker) regulated the temperature in experiments with liquid nitrogen.

Reproducibility

In qualitative terms the chronological succession of individual spectra of the generated radicals is well reproducible. However, in quantitative terms the yield of the individual radicals in the same time scale frequently differs due to the reaction rates, which are a very sensitive function of various parameters, such as concentration ratios, bubbling with air, argon or oxygen, the escape of H_2S, the pH of the solutions and others as well. The most representative sets of experiments were considered in the evaluations below, as illustrated with some original records in Figures 2 and 5.

Evaluations

The detected EPR spectra were analysed and simulated employing Bruker software *Win*EPR and *SimFonia*, and the *Winsim2002* software freely available from the website of the National Institute of Environmental Health Sciences (NIEHS) (http://epr.niehs.nih.gov/) [36].

Results and discussion

Antioxidant properties of NaHS

Substantial differences were found in the antioxidant behaviour of NaHS when working under argon or with air-saturated solutions. Figure 1 presents the results obtained using DPPH (Figure 1A) and $ABTS^{\bullet +}$ (Figure 1B) radicals as oxidants. The relative concentrations of DPPH and $ABTS^{\bullet +}$ radicals monitored *in situ* 10 minutes after the preparation of the sample in the EPR cavity, decreased with increasing $\frac{c_{0,\mathrm{NaHS}}}{c_{0,\mathrm{oxidant}}}$ ratios, where $c_{0,\mathrm{NaHS}}$ and $c_{0,\mathrm{oxidant}}$ represent the initial concentration of reactants. In experiments performed under argon, applying buffered aqueous solutions (pH = 7), well-shaped dependencies with sharp equivalence points were obtained, indicating that approximately one molecule of NaHS (representing an H_2S/HS^- couple) terminated one molecule of oxidant radical (DPPH or $ABTS^{\bullet +}$). A substantially different behaviour was found under air, as compared to argon, where no sharp equivalent points were evident for either oxidant, even at such high NaHS ratios as $\frac{c_{0,\mathrm{NaHS}}}{c_{0,\mathrm{oxidant}}} = 5$ (Figure 1). Additionally, in air-saturated solutions, the antioxidant activity of NaHS monitored with DPPH is much lower than that observed with $ABTS^{\bullet +}$. The impairment of the antioxidant activity in aerated solutions certainly reflects the competitive reactions of oxygen originating from air with NaHS. Thus, the amount of oxidant radicals terminated by NaHS in aerated solution was lower, as compared to experiments under argon. The higher impairment by the antioxidant action of DPPH in comparison to $ABTS^{\bullet +}$ in aerated solutions may partly result from different reaction mechanisms of these oxidants, but probably also from the higher oxygen solubility in the mixed water-ethanol solvent as compared with pure water [37], thus increasing the competitive reaction of oxygen. The mixed solvent had to be used, due to the low solubility of DPPH in water [35].

As molecular oxygen evidently played a dominant role in the reactions of NaHS, we focused our further investigations on the participation of oxygen in NaHS radical reactions. The investigations were carried out under air and/or argon atmosphere in the presence of two different spin trapping agents (DMPO and DBNBS), using both protolytic (H_2O) and aprotic (DMSO) solvents.

NaHS dissolved in H_2O in the presence of DMPO

Figure 2A shows the formation of radical adducts monitored after mixing of the air-saturated 0.1 M

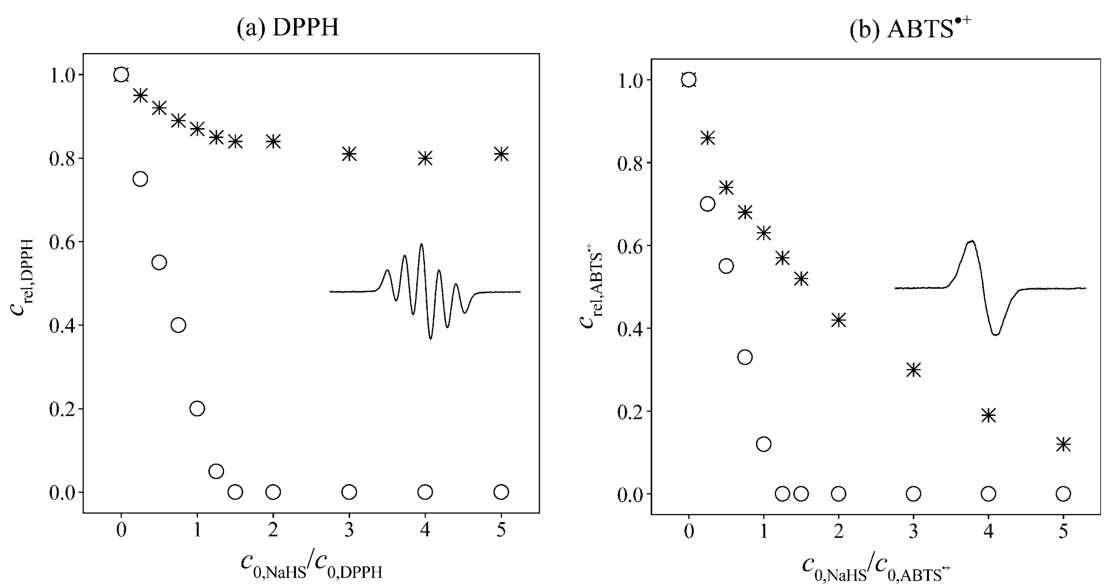

Figure 1. Antioxidant effect of NaHS investigated (A) in 50 μM DPPH aqueous-ethanol (50 % v/v) and (B) in 50 μM $ABTS^{\bullet +}$ aqueous solutions under argon (○) and on air (*). The relative concentrations, c_{rel}, of oxidant radicals DPPH and $ABTS^{\bullet +}$ (their EPR spectra are presented as insets) are quoted upon the increased initial concentration ratios NaHS:DPPH and NaHS:$ABTS^{\bullet +}$, respectively.

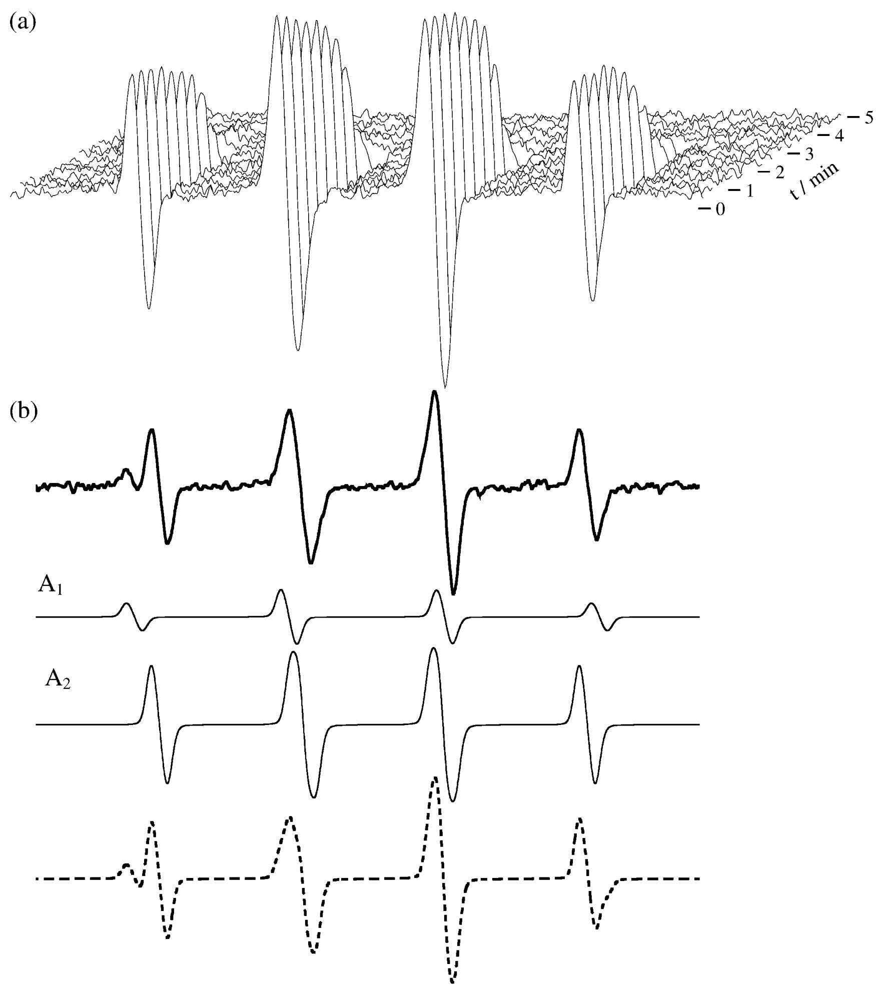

Figure 2. (A) Time monitoring of DMPO adducts formed in 0.1 M NaHS, 0.1 M DMPO aerobic aqueous solution (no radical formation under argon). Repeated bubbling with air reproduces an analogous time evolution of EPR spectra, as presented in (A). (B) Experimental (—) and simulated (---) EPR spectra (SW = 8 mT) extracted from (A) as monitored after 3 min reaction time, simulated as a sum of two spectra ($A_1 + A_2$): A_1 with $a_N = 1.635$ mT, $a_H^\beta = 1.613$ mT; g = 2.0056 with share of 19.9% assigned to $^\bullet$DMPO-S$^-$ and A_2 with $a_N = 1.465$ mT, $a_H^\beta = 1.563$ mT; g = 2.0055 with a share of 80.1% attributed to $^\bullet$DMPO-SO_3^- adduct.

NaHS with 0.1 M DMPO neutral solutions (pH = 7, phosphate buffer). No radicals were observed in analogous experiments under argon, documenting the central role of oxygen in the formation of radicals. The maximal concentration of radical adducts was found immediately after mixing of the reactants under air. In the later stages of the experiment their concentration continuously diminished and adducts vanished completely after 8 minutes. If such a solution was re-saturated with air, EPR spectra identical to those shown in Figure 2A, with an analogous diminishing pattern, were observed. This procedure of air bubbling could be reproduced numerous times with the same result. The observed behaviour indicates a reaction of oxygen from air with NaHS, leading to the formation of the radical adducts, which are later terminated in the NaHS system. This suggestion was supported by an additional experiment (data not shown), in which $^\bullet$DMPO-OH adducts generated by the UV irradiation of H_2O_2 in the presence of DMPO spin trap rapidly vanished after the addition of NaHS into the solution. This explains the relatively rapid vanishing of the radical adducts presented above in the NaHS system (Figure 2A), as a process of their generation, time-limited due to the oxygen concentration present in the solution, coupled with their termination by NaHS or its products. The reaction of oxygen and its continuous vanishing during the reaction were monitored with the TEMPOL probe as described in more detail in experiments presented below using DMSO solvent.

A representative experimental EPR spectrum A_1, along with its simulation, is shown in Figure 2B. The spectrum was extracted from Figure 2A as the third scan and simulated as a sum of two spectra ($A_1 + A_2$) with the following spin Hamiltonian parameters: A_1 with $a_N = 1.635$ mT, $a_H^\beta = 1.613$ mT; g = 2.0056 with share of 19.9% and A_2 with $a_N = 1.465$ mT, $a_H^\beta = 1.563$ mT; g = 2.0055 with share of 80.1%. According to the literature [30,38,39], the spectrum A_1 can be assigned to sulphide radical anion ($^\bullet S^-$)

added to DMPO, given that sulphide radical anions most probably dominate in neutral aqueous solutions ($HS^{\bullet} \rightleftharpoons S^{\bullet -} + H^{+}$) [40].

The assignment of a radical trapped by DMPO producing the spectrum A_2 is more complex. According to data in the literature, numerous reports are available on the sulphide reactions, including its spontaneous oxidation in sea waters [30] and biological systems [29]. However, we shall focus on some initial steps of the reactions and species, which may be reflected in our EPR study. The most frequently proposed primary reaction step in the presence of oxygen is the electron transfer from NaHS to oxygen [29,30,41] under the formation of sulphhydryl radical $HS^{\bullet}/S^{\bullet -}$ and superoxide radical anion $O_2^{\bullet -}$, according to equation (2):

$$HS^{-} + O_2 \rightarrow HS^{\bullet} + O_2^{\bullet -} \quad (2)$$

No direct confirmation of the superoxide radical anion formation with HS^{-} is available so far. There are various further steps and routes for the formed sulphhydryl radical and superoxide radical anions considered in accordance with data in the literature, which are summarized in Table I. In general, superoxide radical anion in aqueous solutions rapidly protonates to perhydroxyl radical $HO_2^{\bullet}$, enters consecutive reactions resulting in the formation of $^{\bullet}OH$ radicals, which can readily react with H_2S/HS^{-} producing sulphhydryl radicals [40].

Table I. Individual reactions with the corresponding bimolecular rate constants reported for aerobic aqueous sulphidic systems.

Reaction	$M^{-1}s^{-1}$	pH	Reference
$O_2^{\bullet -} + H^{+} \rightleftharpoons HO_2^{\bullet}$	5×10^{10}	4	[51]
$HO_2^{\bullet} + O_2^{\bullet -} + H_2O \rightarrow H_2O_2 + O_2 + OH^{-}$	9.7×10^{7}		[52]
$HO_2^{\bullet} + HO_2^{\bullet} \rightarrow H_2O_2 + O_2$	8.3×10^{5}		[52]
$H_2O_2 + O_2^{\bullet -} \rightarrow {}^{\bullet}OH + O_2 + OH^{-}$	1.3×10^{-1}	7–9.9	[53]
$H_2S/HS^{-} + {}^{\bullet}OH \rightarrow HS^{\bullet}/S^{\bullet -} + H_2O$	$\sim 10^{10}$		[40]
$S^{\bullet -} + HS^{-} \rightarrow HS_2^{\bullet 2-}$	4.0×10^{9}		[54]
$HS^{\bullet} + HS^{-} \rightarrow H_2S_2^{\bullet -}$	—		[40]
$HS^{\bullet} + HS^{\bullet} \rightarrow H_2S_2$	6.5×10^{9}	7	[55]
$H_2S_2^{\bullet -} + O_2 \rightarrow H_2S_2 + O_2^{\bullet -}$	4.0×10^{8}	7	[55]
$HS^{\bullet} + O_2 \rightarrow HSO_2^{\bullet}$	7.5×10^{9}	7	[55]
$HS^{\bullet} + O_2 \rightarrow SO_2^{\bullet -} + H^{+}$	7.5×10^{9}	7	[55]
$HSO_2^{\bullet} \rightleftharpoons H^{+} + SO_2^{\bullet -}$	—		[30]
$SO_2^{\bullet -} + O_2 \rightarrow SO_2 + O_2^{\bullet -}$	1×10^{8}	6.5	[56]
$2\ SO_2^{\bullet -} \rightarrow S_2O_4^{2-}$	1.7×10^{9}	6.5	[56]
$SO_2 + H_2O \rightarrow HSO_3^{-} + H^{+}$	—		[57]
$HSO_3^{-} + {}^{\bullet}OH \rightarrow SO_3^{\bullet -} + H_2O$	4.5×10^{9}		[58]
$2\ HS^{-} + 4\ HSO_3^{-} \rightarrow 3\ S_2O_3^{2-} + 3\ H_2O$	—		[57]
$S_2O_4^{2-} + O_2 + H_2O \rightarrow HSO_3^{-} + HSO_4^{-}$	—		[57]
$2\ S_2O_4^{2-} + H_2O \rightarrow 2\ HSO_3^{-} + S_2O_3^{2-}$			[57]
$2\ SO_3^{2-} + O_2 \rightarrow 2\ SO_4^{2-}$			[57]
$SO_3^{\bullet -} + O_2 \rightarrow SO_5^{\bullet -}$	1.5×10^{9}		[59]
$2\ SO_5^{\bullet -} \rightarrow S_2O_8^{2-} + O_2$	1×10^{8}	6	[60]
$SO_5^{\bullet -} + HSO_3^{-} \rightarrow SO_3^{\bullet -} + HSO_5^{-}$	3.6×10^{3}		[61]

Previously, Tapley et al. [30] investigated sulphide reactions in a system (sulphide in sea waters) analogous to ours and suggested the formation of hydroxyl and sulphite radicals. An alternative, in the presence of oxygen, is that the radicals $HS^{\bullet}/S^{\bullet -}$ together with oxygen form sulphur dioxide radical anion $SO_2^{\bullet -}$ (as proposed in [41,42]), which in further consecutive reactions lead to a variety of oxygenated sulphur paramagnetic intermediates [42], i.e. sulphur- or oxygen-centred radicals generally named here $\{S_xO_y\}^{\bullet}$ (Table I). Concerning our reaction system ($NaHS/H_2O/O_2/DMPO$), sulphite radical anions generated from the sulphhydryl route were probably added to DMPO (equation 3) and observed as radical A_2.

$$SO_3^{\bullet -} + DMPO \rightarrow {}^{\bullet}DMPO\text{-}SO_3^{-} \quad (3)$$

The assumed sulphite formation is in good agreement with previous investigations on $SO_2^{\bullet -}$ radical spin trapping by nitrones, where a bimolecular reaction of $SO_2^{\bullet -}$ with the DMPO molecule was evidenced, coupled with the formation of $^{\bullet}DMPO\text{-}SO_3^{-}$ spin adduct in the presence of mild oxidants [43]. The spin Hamiltonian parameters of A_2 found here are in good correlation with the data so far published [38,44–48] on sulphite radical anion added to DMPO, $^{\bullet}DMPO\text{-}SO_3^{-}$. The rapid reaction of sulphite radical anion with molecular oxygen, through consecutive reactions, can produce sulphate radical anions or hydroxyl radicals [49,50].

NaHS dissolved in DMSO in the presence of DMPO

The choice of DMSO solvent was motivated by the general experience that the formation of a superoxide radical anion may be well documented by spin trapping in DMSO solvent. No radical formation was observed when experiments were carried out under argon, similarly to the experiments in water (data not shown). The results obtained in aerated DMSO solutions are summarized in Figure 3. A 10 mM NaHS solution prepared under argon and 30 mM DMPO under air were simultaneously inserted via a small mixing chamber into the flat cell placed in the EPR cavity and the monitoring of radical formation started immediately. Two EPR spectra B_1 and B_2 (Figure 3A and B) were observed during the 10 min-monitoring of the reaction. Their intensities varied with time, as shown in Figure 3C. The time-course of both spectra suggests a consecutive reaction: the rapid formation of radical adduct B_1 followed by its continuous diminution given the simultaneous increase of B_2. The EPR signals of both radical adducts vanished completely after 10 min. Then, similarly to what was already observed above in aqueous solutions, if the solution was bubbled with air the radical adduct

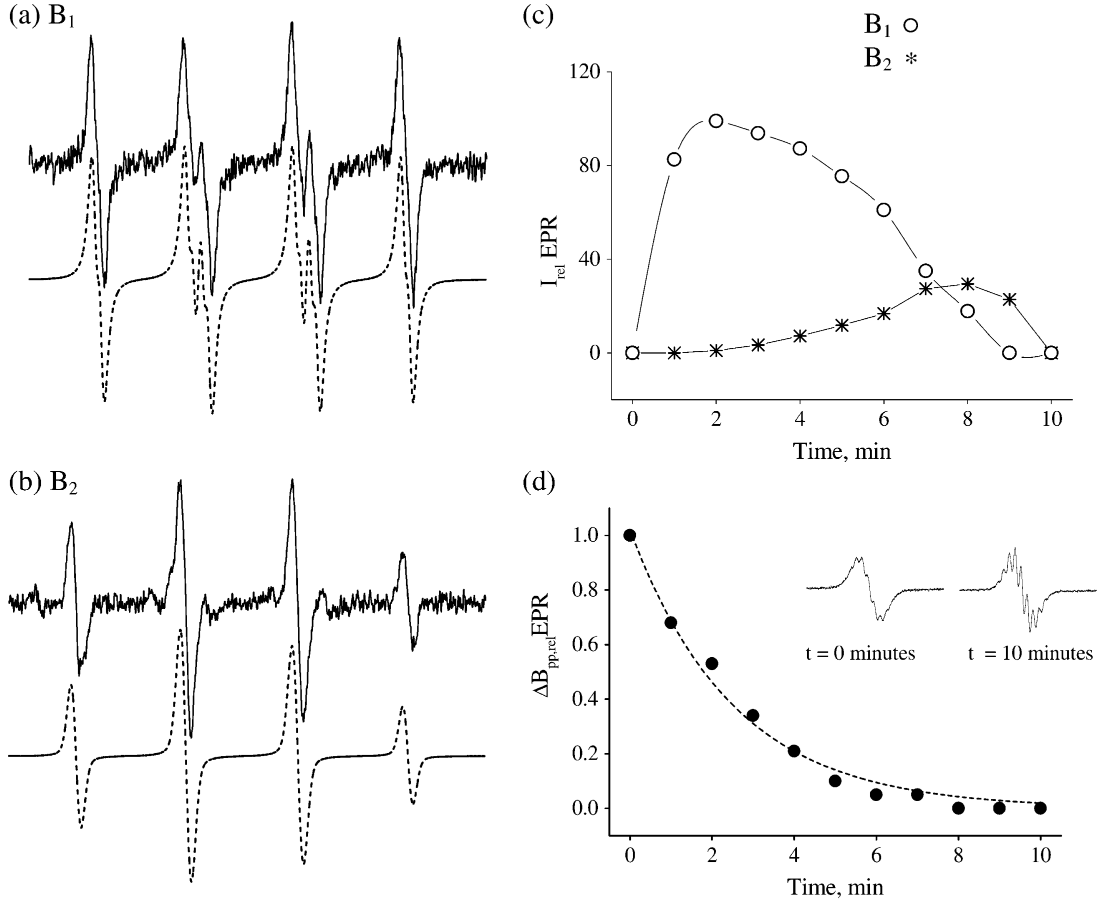

Figure 3. (A, B) Experimental (—) and simulated (---) EPR spectra B_1, B_2 as monitored over 10 min after mixing equal volumes of 10 mM NaHS solution prepared under argon with 30 mM DMPO solution saturated with oxygen, both in DMSO solvent. Spectrum B_1 was extracted as the second scan and spectrum B_2 as the last but one scan. Simulation parameters are: B_1 with $a_N = 1.37$ mT, $a_H^{\beta} = 1.175$ mT, $a_H^{\gamma} = 0.083$ mT; g = 2.0056 and B_2 with $a_N = 1.36$ mT and $a_H^{\beta} = 1.31$ mT; g = 2.0055. Spectrum was B_1 tentatively assigned to $^{\bullet}$DMPO-SH adduct and B_2 to the radicals of oxidized sulphides $\{S_xO_y\}^{\bullet}$ added to DMPO. (C) The change of relative intensities I_{rel}, of EPR spectra B_1 and B_2 quoted upon the time resulting in an EPR silent system after 10 min. After saturation of the thus obtained EPR silent solution with air, the pattern of spectra presented in (C) can be well reproduced again. (D) Working under conditions analogous to (C) in the presence of TEMPOL the decrease of its relative line widths $\Delta B_{pp,rel}$ maps the decreasing concentration of oxygen dissolved. Insets present EPR spectra of the investigated solution saturated with air ($t = 0$ min) and its changes after 10 min reaction time ($t = 10$ min). The spectrum with $t = 10$ min corresponds well to the TEMPOL spectrum under argon, thus indicating the total consumption of oxygen from air by NaHS.

formation and decay shown in Figure 3A and B could be reproduced numerous times.

The oxygen concentration in the NaHS system was monitored following the changes of the line widths in the EPR spectra of the TEMPOL radical. The line width (reflecting the interaction between TEMPOL and oxygen) increases with the oxygen concentration. We performed an experiment analogous to that described in Figure 3C, where DMPO was replaced with 1 mM TEMPOL and mixed with a 10 mM NaHS solution under air. TEMPOL enters reactions in the NaHS/DMSO/O_2 system [62], but due to its high applied initial concentration, the decrease of its integral EPR intensity was here insignificant. The relative EPR line widths of TEMPOL ($\Delta B_{pp,rel}$) that we evaluated decreased with time, as shown in Figure 3D. To illustrate the changes in the TEMPOL spectrum, the insets in Figure 3D shows one spectrum observed at the beginning of the experiment ($t = 0$ min), which had widely broadened lines, and documents the presence of oxygen at high concentrations. Then, the second spectrum, monitored at the end of the reaction ($t = 10$ min), shows relatively sharp lines, resulting from the narrowing of its line width. This second spectrum corresponds well to the TEMPOL spectrum obtained under argon and indicates the total consumption of oxygen originating from the air in the presence of NaHS. The monitored changes of the TEMPOL spectrum can be stably repeated, if the solution obtained at the end of the monitoring is saturated with air again. The oxygen consumption in Figure 3D correlates well with the radical formation described in Figure 3C. The maximal radical formation is coupled with the highest oxygen drop and the radical formation stays out after oxygen availability ends.

Spectra B_1 and B_2 presented in Figure 3A and B were well simulated, employing the following hyperfine

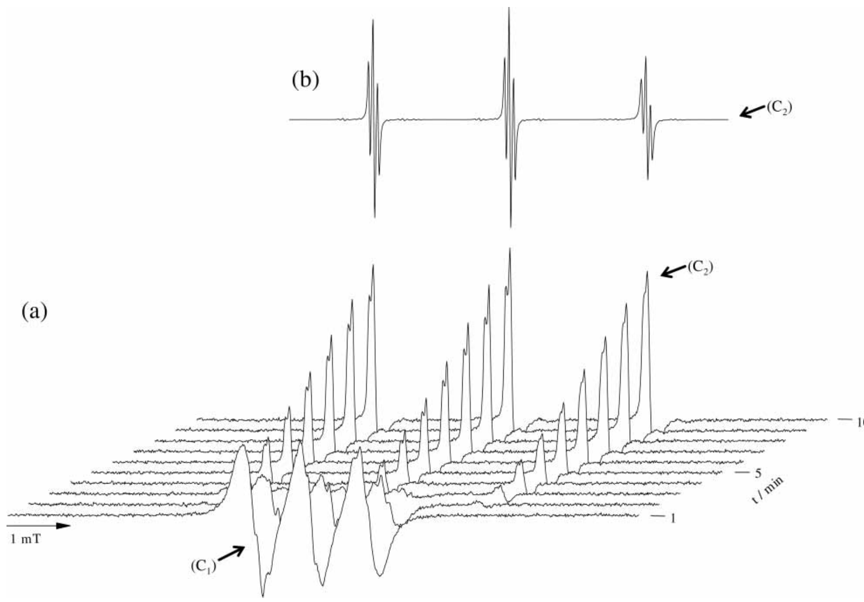

Figure 4. (A) EPR spectra monitored for 10 min after mixing 0.1 M NaHS and 0.1 M DBNBS aqueous solutions under argon. (B) A detailed view of the final spectrum. The first spectrum (C_1) is assigned to the radical anion of spin trap DBNBS$^{\bullet -}$ and the second (C_2) to $S^{\bullet -}$ added to DBNBS ($^{\bullet}$DBNBS-S^-). For simulation parameters see Table II and the details of C_2 in Figure 5.

splittings: radical adduct B_1 with $a_N = 1.37$ mT, $a_H^{\beta} = 1.175$ mT, $a_H^{\gamma} = 0.083$ mT; g = 2.0056 and B_2 with $a_N = 1.36$ mT and $a_H^{\beta} = 1.31$ mT; g = 2.0055. Spectrum B_1 of the first observable adduct to DMPO was expected to originate from superoxide radical anion, $O_2^{\bullet -}$ or sulphhydryl radical $HS^{\bullet}$, which are most probably formed as the primary product in the reaction of HS^- with oxygen, as indicated in equation (2). However, the simulation parameters of B_1 substantially deviate from those reported in the literature in DMSO solvent for $^{\bullet}$DMPO-O_2^- adducts (e.g. $a_N = 1.275$,T, $a_H^{\beta} = 1.035$ mT, $a_H^{\gamma} = 0.135$; g = 2.0057) [63–67]. Therefore, neither B_1 nor B_2 is likely to represent superoxide radical anion spin adduct with DMPO.

As the detection of superoxide radical anion by the spin trapping technique was not effective, probably due to a rapid consecutive reaction of O_2^- or the termination of its DMPO adducts in the NaHS system [68], we tried a different route to detect the superoxide radical anion. The relatively good stability of O_2^- in DMSO is known, and by lowering the temperature down to 160 K, it can be well identified with a characteristic EPR spectrum [69]. Even such an experiment (preparing NaHS solution under argon and mixing with oxygen containing DMSO solutions, dropping the temperature to 160 K) did not bring the expected evidence for the presence of O_2^-. Otherwise we readily obtained a typical EPR spectrum of O_2^- at 160 K from KO_2 dissolved in DMSO. However, if NaHS was added to such a system, the spectrum vanished, documenting the above-assumed possibility, that O_2^- may be terminated in the NaHS system.

However, in numerous literature reports, so far without unambiguous evidence, the formation of O_2^- is proposed; for the reason given above we also assume that in the primary step NaHS donates an electron to molecular oxygen forming intermediately superoxide radical anion (equation 2).

As the spectrum of the primary formed adduct B_1 is not compatible with $^{\bullet}$DMPO-O_2^-, another alternative remains of assigning B_1 to the adduct of sulphhydryl radical $HS^{\bullet}$ formed in the primary reaction step (equation 2), since in DMSO solutions NaHS is practically completely dissociated into free ions [70]. This appears very probable, as under analogous conditions using DBNBS spin trap in DMSO instead of DMPO (described below), evidence for the -SH group added to the spin trap was confirmed in the presence of deuterated water. The radical B_1 with hyperfine splittings $a_N = 1.37$ mT, $a_H^{\beta} = 1.175$ mT, $a_H^{\gamma} = 0.083$ mT represents an acceptable alternative for $^{\bullet}$DMPO-SH adduct.

Adduct B_2, consecutively formed after B_1, probably originates from oxidized sulphhydryl radicals, namely $^{\bullet}$DMPO-$\{S_xO_y\}$, as already discussed above (Table I).

Sulphite adduct $^{\bullet}$DMPO-SO_3^- remains out of consideration, since the hyperfine splittings of B_2 differ substantially from the data published previously for $^{\bullet}$DMPO-SO_3^- in DMSO solvent [71].

NaHS dissolved in water in the presence of DBNBS

Representative time-dependent EPR spectra of the sample after mixing 0.1 M NaHS with 0.1 M DBNBS under argon are shown in Figure 4. Similar spectra were obtained in aerated solutions, indicating that the primary reactant for NaHS is not necessarily just molecular oxygen, but in this case the DBNBS spin trap also, under argon. The three-line EPR

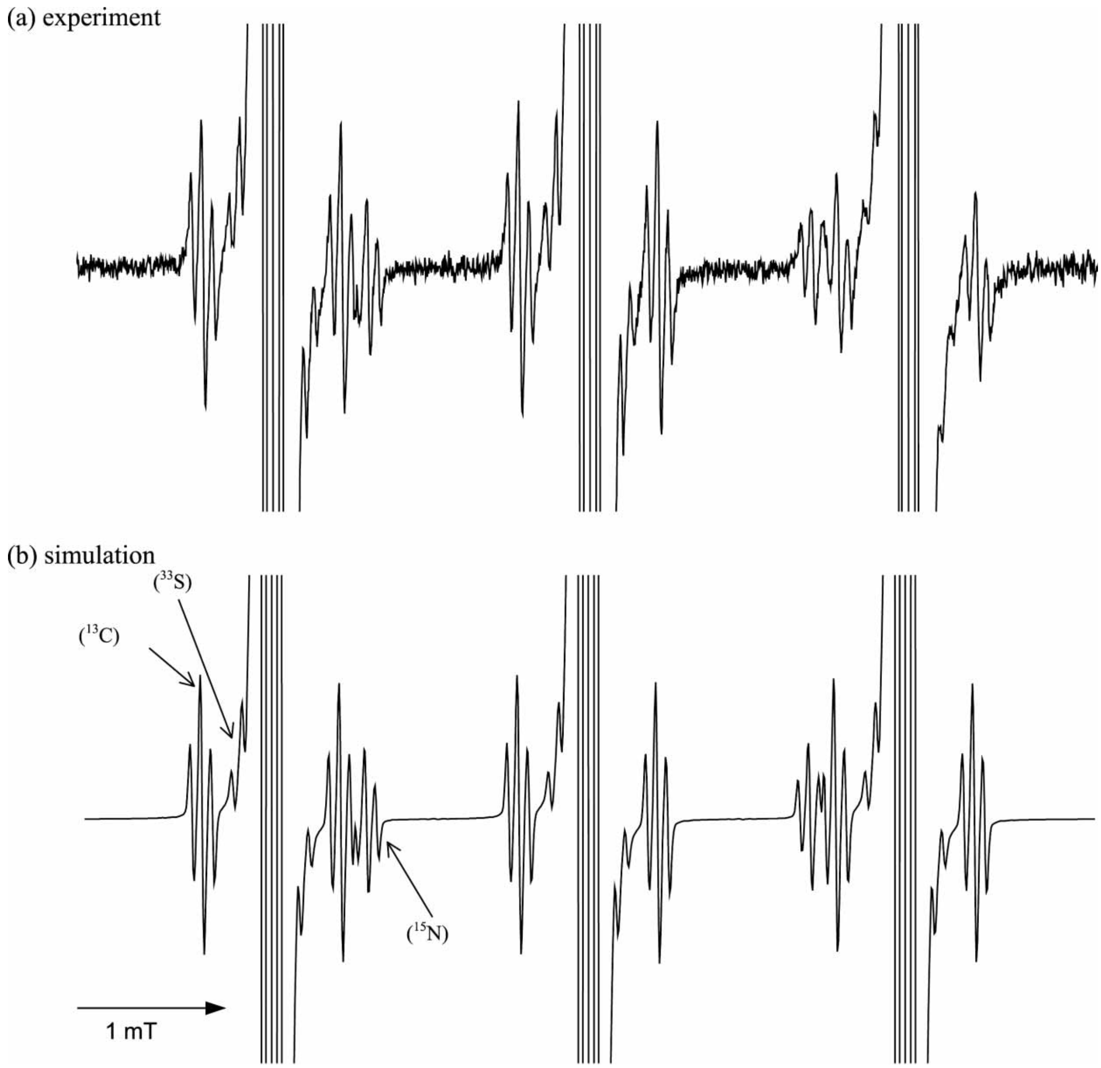

Figure 5. A detailed view of the experimental (A) and simulated (B) EPR spectra of radical species C_2 obtained from Figure 4, mixing anaerobic aqueous solutions of 0.1 M NaHS with 0.1 M DBNBS. The simulation parameters of C_2 are: $a_N = 2.17$ mT $a_H(2H^{meta}) = 0.07$ mT and satellite splittings $a_N(^{15}N) = 3.04$ mT, $a_S(^{33}S) = 0.128$ mT, and $a_C(^{13}C) = 0.95$ mT.

spectrum (C_1) typical for the interaction of an unpaired electron with a ^{14}N nucleus with $a_N = 0.92$ mT, $g = 2.0070$ plus further not-well-resolved splittings dominate in the primary stage of the experiment. The EPR signal C_1 quickly decayed and was replaced by the spectrum C_2 (Figure 4B). The well-resolved satellite pattern, with detailed analysis, is shown in Figure 5.

Spectrum C_1 is assigned to the radical anion of DBNBS spin trap, based on our electrochemical investigations (not presented), where in the reversible one-electron reduction of DBNBS in water, a radical species with a closely analogous EPR spectrum was found. Such a DBNBS radical anion can be formed in the presence of NaHS by an electron transfer from sulphide HS^- to DBNBS according to equation (4):

$$H_2S/HS^- + DBNBS \rightarrow HS^{\bullet}/S^{\bullet -} + DBNBS^{\bullet -} + H^+ \quad (4)$$

Additionally, in the aerated aqueous solution, an alternative path of $DBNBS^{\bullet -}$ generation can also be proposed (equation 5) [72], resulting in the enhanced $DBNBS^{\bullet -}$ formation observed in aerobic solution, as compared to the experiments under argon.

$$O_2^{\bullet -} + DBNBS \rightarrow O_2 + DBNBS^{\bullet -} \quad (5)$$

Spectrum C_2 was simulated with hyperfine splittings $a_N = 2.17$ mT, $a_H(2H^{meta}) = 0.07$ mT, $g = 2.0058$, and we assign it to the $HS^{\bullet}/S^{\bullet -}$ adduct of DBNBS, based on the following data. The reaction was carried out under argon in NaHS/H_2O/DBNBS solution. DBNBS spin trap is the only potential acceptor available for the HS^- donor in this system. Formation of its radical anion was confirmed above and is actually coupled with the formation of sulphhydryl radicals. Therefore, a straightforward alternative is the addition of so formed $HS^{\bullet}$ to DBNBS nitroso spin trap under the formation of $^{\bullet}$DBNBS-SH (equation 6). The

Table II. An overview of radicals (R) formed and hyperfine splitting constants extracted from their EPR spectra observed as spin adducts in the reaction of NaHS in the presence of two spin traps (DMPO and DBNBS) in two various solvents (H_2O and DMSO) under argon or in the presence of oxygen.

R	Confirmed [suggested]	Hyperfine splitting (mT)	System
A_1	$^•$DMPO-S^-	$a_N = 1.635$; $a_H^{\beta} = 1.613$	NaHS/DMPO/H_2O/O_2
A_2	$^•$DMPO-SO_3^-	$a_N = 1.465$; $a_H^{\beta} = 1.563$	
B_1	$^•$DMPO-[SH]	$a_N = 1.37$; $a_H^{\beta} = 1.175$; $a_H^{\gamma} = 0.083$	NaHS/DMPO/DMSO/O_2
B_2	$^•$DMPO-[{S_xO_y}]	$a_N = 1.36$ mT; $a_H^{\beta} = 1.31$	
C_1	DBNBS$^{•-}$	$a_N = 0.92$	NaHS/DBNBS/H_2O/Ar or O_2
C_2	$^•$DBNBS-[S^-]	$a_N = 2.17$; $a_H(2H^{meta}) = 0.07$ satellites $a_N(^{15}N) = 3.04$; $a_S(^{33}S) = 0.128$; $a_C(^{13}C) = 0.95$	NaHS/DBNBS/H_2O/O_2
C_3	$^•$DBNBS-SO_3^-	$a_N = 1.26$; $a_H(2H^{meta}) = 0.062$ satellites* $a_N(^{15}N) = 1.765$; $a_S(^{33}S) = 0.178$; $a_C(^{13}C_{2,6}) = 0.832$; $a_C(^{13}C_1) = 0.655$	NaHS/DBNBS/H_2O/O_2 after 12-h sulphite formation
D_1	$^•$DBNBS-SH	$a_N = 0.88$; $a_H(2H^{meta}) = 0.125$; $a_H(SH) = 0.26$	NaHS/DBNBS/DMSO/Ar or O_2
D_2	DBNBS$^{•-}$	$a_N = 0.61$; $a_H(2H^{meta}) = 0.116$;	
D_3	$^•$DBNBS-SD	$a_N = 0.88$; $a_H(2H^{meta}) = 0.125$; $a_D(SD) = 0.04$	

*According to [73].

missing proton interaction from the HS group may be explained by its dissociation to sulphidic anion $^•$DBNBS-S^-.

$$HS^•/S^{•-} + DBNBS \rightarrow {}^•DBNBS\text{-}S^- + H^+ \qquad (6)$$

A further support for such an assignment is obtained from experiments described above with an analogous system (NaHS/DMPO/H_2O). DMPO there was replaced here with DBNBS. In the DMPO system, the sulphhydryl radical was identified as $^•$DMPO-S^- adduct. As both systems differ only in the spin trap present, we assume that identical sulphhydryl radicals ($HS^•/S^{•-}$) are formed and added to both spin traps. This implies here the formation of $^•$DBNBS-S^-.

The highly-resolved EPR spectrum C_2 from Figure 4 reveals satellite splittings as presented in Figure 5. It was simulated with: $a_N = 2.17$ mT $a_H(2H^{meta}) = 0.07$ mT and satellite splittings $a_N(^{15}N) = 3.04$ mT, $a_S(^{33}S) = 0.128$ mT and $a_C(^{13}C) = 0.95$ mT. The evidence of a sulphur satellite with $a_S(^{33}S) = 0.128$ mT in spectrum C_2 is similar to $a_S(^{33}S) = 0.178$ mT observed in spectrum C_3, assigned to sulphite radical anion adduct. The sulphur in C_3 is directly bonded to the nitroxi group ($^•$ON-S). Consequently, an analogous constellation, namely an addition of a sulphur-centred radical to the nitroso spin trap DBNBS is expected in C_2 radical. If a 0.2 M NaHS solution was exposed to air for 12 h and then DBNBS added, a spin trap adduct C_3 was observed. It was well simulated with hyperfine splittings (Table II: C_3), already published by Stolze and Mason [73], for sulphite added to DBNBS ($^•$DBNBS-SO_3^-). Therefore it is to be assumed that NaHS here is oxidized to sulphite in good accordance with the results found with DMPO [74,75].

NaHS dissolved in DMSO in the presence of DBNBS

A relatively high concentration of radical D_1 (Figure 6A) was observed during the first 42-s scan commencing instantly after mixing the 0.02 M NaHS with 0.02 M DBNBS in DMSO solutions under argon. In the second scan a further spectrum of radical D_2 (Figure 6B) is clearly evident under a progressive vanishing of D_1. Both spectra vanished completely in the next scans. We assign D_1 to $HS^•$ radical added to DBNBS and D_2 to the radical anion of spin trap DBNBS$^{•-}$. This is based on the following data. Considering again the components present in the solutions (NaHS/DBNBS/DMSO) under argon, DBNBS is the only available potential acceptor for the HS^- donor. Thus, electron transfer from HS^- to DBNBS is taking place under the formation of $HS^•$ and DBNBS$^{•-}$ radicals, as already formulated above (equation 4). Radical $HS^•$ formed there is then stabilized as $^•$DBNBS-SH adduct (equation 6), evident as D_1.

The suggested assignment of D_1 was confirmed in an additional experiment analogous to that presented in Figure 6A, where deuterated water D_2O was added (giving 1 M D_2O solution in DMSO), obtaining spectrum D_3 (Figure 6C). The simulation parameters of both spectra (D_1 and D_3) reveal the same hyperfine splittings originating from the DBNBS skeleton (nitroxi group with $a_N = 0.86$ mT and two protons from benzene ring with $a_H(2H^{meta}) = 0.125$ mT, Table II). A further splitting evident in D_1, with $a_H(SH) = 0.26$ mT, was assigned to the hydrogen from $^•$SH added to DBNBS, since the experiment with deuterated water brought the expected changes of $a_H(SH) = 0.26$ mT in D_1 to $a_D(SD) = 0.04$ mT in D_3 (Figure 6C). The assignment of D_2 to DBNBS$^{•-}$ is based on our electrochemical reduction of DBNBS in DMSO solvent, where the radical anion with an analogous

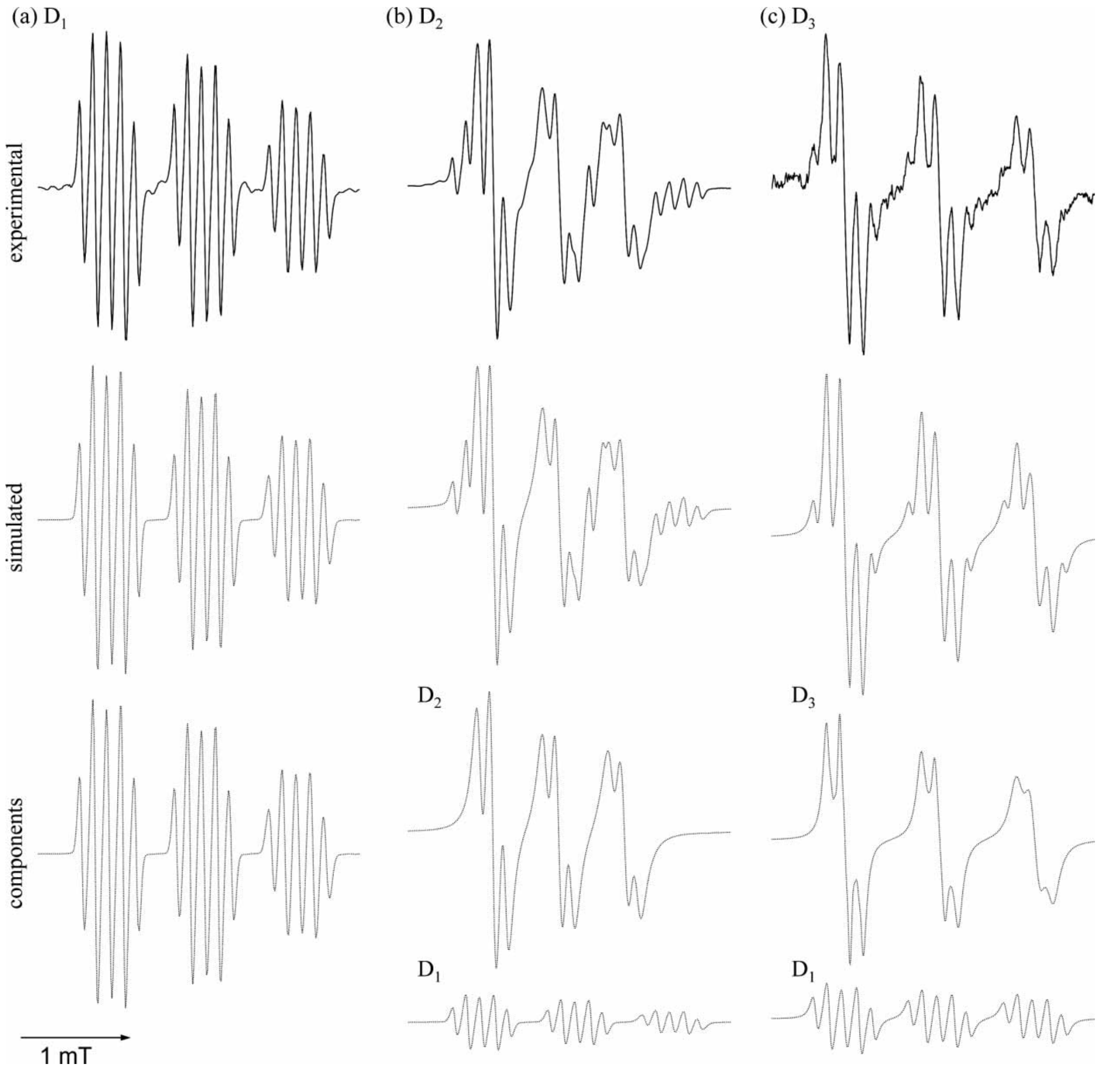

Figure 6. Experimental and simulated EPR spectra observed in 0.02 M NaHS, 0.02 M DBNBS solution in DMSO under argon. (A) D_1 represents $HS^{\bullet}$ radical adduct to DBNBS observed during the first 42-s scan. (B) D_2, observed as the second scan, was assigned to radical anion of spin trap $DBNBS^{\bullet -}$. Spectrum D_3 confirms $HS^{\bullet}$ radical adduct formation D_1, where in an analogous experiment to (A) in the presence of deuterated water the expected change of a_H(SH) to a_D(SD) splitting was observed. For simulation parameters see Table II.

EPR spectrum to that presented by D_2 was observed (Table II) as a primary reversible reduction product.

The NaHS/DBNBS/DMSO reaction system produced a large variety of radicals, if saturated with air (not presented). A similar experience of a variety of radicals was reported by Stolze and Mason [73] when investigating the alkaline/DMSO/DBNBS system. We assume that, as discussed above, $\{S_xO_y\}^{\bullet}$ radicals of oxidized sodium hydrosulphide are added to DBNBS here. The sulphite radical DBNBS adduct ($^{\bullet}$DBNBS-SO_3^-) remains the only definitely identified product in the NaHS/DMSO solution exposed to air for 12 h, similarly to what was described above in aqueous solutions.

Conclusions

The H_2S/HS^- system frequently referred to in the literature and well represented with NaHS in neutral (pH = 7) solution was investigated in detail by EPR spectroscopy. Sodium hydrosulphide (donor of H_2S/HS^-) acts as an effective antioxidant and terminates DPPH and $ABTS^{\bullet +}$ radical oxidants up to a stoichiometric ratio of 1:1 under argon. The antioxidant activity is substantially lowered by the competitive reaction of NaHS with molecular oxygen, if present in the system.

Systematic investigations of NaHS in its function as an electron donor were carried out. Two different types of spin trapping agents (DMPO, DBNBS) in protolytic and aprotic (H_2O, DMSO) solvents under an argon or an oxygen atmosphere were employed. An overview of the radicals observed and the data extracted from their EPR spectra is presented in Scheme 1 and Table II. Electron acceptors such as O_2 or the spin trap DBNBS were necessary to initiate the NaHS radical reactions. The formation of sulphhydryl radicals ($S^{\bullet -}$ predominates in aqueous solvents

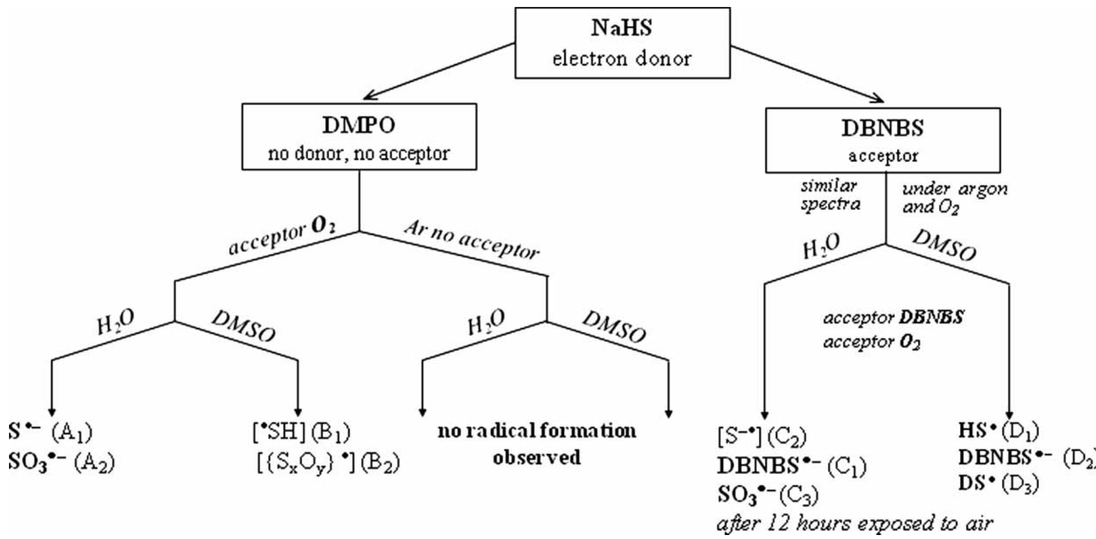

Scheme 1. Sodium hydrosulphide in its function as electron donor followed with two spin traps (DMPO, DBNBS) in two different solvents (H_2O, DMSO) under oxygen or under argon. Radicals confirmed or [suggested] as corresponding spin adducts are marked below.

and $HS^{\bullet}$ in DMSO) and radical anions of spin trap DBNBS were confirmed. The expected formation of superoxide radical anion coupled with the formation of sulphhydryl radicals (equation 2) was implied, but not confirmed, as $^{\bullet}$DMPO-O_2^- spin adduct, probably due to the rapid consecutive reactions of $O_2^{\bullet-}$ or the low stability of its adduct in the sulphidic system. No radical formation was indicated in the presence of NaHS with DMPO spin trap under argon, evidently due to the missing electron acceptor in the system. Sulphhydryl radicals in the presence of molecular oxygen rapidly form further unidentified paramagnetic radical intermediates $\{S_xO_y\}^{\bullet}$, e.g. the sulphite radical adducts ($^{\bullet}$DMPO-SO_3^- and $^{\bullet}$DBNBS-SO_3^-) were found in NaHS solutions exposed to air.

These results may contribute to understanding numerous biological effects of H_2S/HS^- particularly in which an oxidative stress is involved, keeping in mind that, due to the electron donor properties, especially in the presence oxygen, sulphides are involved in a variety of reactions. For example, it was reported that H_2S reduced oxidative stress in a model of a myocardial ischemic heart disease [5,76], in a lung and hepatic ischemia–reperfusion injury [77,78], in a H_2O_2-induced neural injury [21], in a rat gastric mucosal epithelium [19] and in brain endothelial and neuronal cells [16,79,80]. H_2S inhibited peroxynitrite-induced cytotoxicity and protein oxidation in human neuroblastoma SH-SY5Y cells [24], hemin-mediated oxidation of low-density lipoprotein [81], superoxide formation in human vascular smooth muscle cells [14] and production of reactive oxygen species in spontaneously hypertensive rats [82].

Acknowledgements

This work was financially supported by the the Scientific Grant Agency of the Slovak Republic (Project VEGA/1/0018/09) and the Research and Development Agency of the Slovak Republic (contract No. APVV-0397-07).

Declaration of interest: The authors report no conflicts of interest. The authors alone are responsible for the content and writing of the paper.

References

[1] Zhao W, Zhang J, Lu Y, Wang R. The vasorelaxant effect of H_2S as a novel endogenous gaseous H_2S channel opener. EMBO J 2001;20:6008–6016.

[2] Geng B, Yang J, Qi Y, Zhao J, Pang Y, Du J, Tang C. H_2S generated by heart in rat and its effects on cardiac function. Biochem Biophys Res Commun 2004;313:362–368.

[3] Johansen D, Ytrehus K, Baxter G. Exogenous hydrogen sulfide (H_2S) protects against regional myocardial ischemia-reperfusion injury—evidence for a role of K_{ATP} channels. Basic Res Cardiol 2006;101:53–60.

[4] Sivarajah A, McDonald M, Thiemermann C. The production of hydrogen sulfide limits myocardial ischemia and reperfusion injury and contributes to the cardioprotective effects of preconditioning with endotoxin, but not ischemia in the rat. Shock 2006;26:154–161.

[5] Chen C, Xin H, Zhu Y. Hydrogen sulfide: third gaseous transmitter, but with great pharmacological potential. Acta Pharmacol Sin 2007;28:1709–1716.

[6] Lowicka E, Beltowski J. Hydrogen sulfide (H_2S)—the third gas for interest for pharmacologists. Pharm Rep 2007;59: 4–24.

[7] Yang G, Wu L, Jiang B, Yang W, Qi J, Cao K, Meng Q, Mustafa A, Mu W, Zhang S, et al. H_2S as a physiologic vasorelaxant: hypertension in mice with deletion of cystathionine gamma-lyase. Science 2008;322:587–590.

[8] Ondrias K, Stasko A, Cacanyiova S, Sulova Z, Krizanova O, Kristek F, Malekova L, Knezl V, Breier A. H_2S and HS^- donor NaHS releases nitric oxide from nitrosothiols, metal nitrosyl complex, brain homogenate and murine L1210 leukaemia cells. Pflugers Arch 2008;457:271–279.

[9] Wang R. The gasotransmitter role of hydrogen sulfide. Antioxid Redox Signal 2003;5:493–501.

[10] Ali M, Ping C, Mok Y, Ling L, Whiteman M, Bhatia M, Moore PK. Regulation of vascular nitric oxide in vitro and in vivo; a new role for endogenous hydrogen sulphide? Br J Pharmacol 2006;149:625–634.
[11] Whiteman M, Li L, Kostetski I, Chu S, Siau J, Bhatia M, Moore PK. Evidence for the formation of a novel nitrosothiol from the gaseous mediators nitric oxide and hydrogen sulphide. Biochem Biophys Res Commun 2006;343: 303–310.
[12] Whiteman M, Ali M, Li L, Cheong Y, Mok Y, Kostetski L, Chu SH, Siau JL, Bhatia M, Moore PK. Hydrogen sulfide regulates the availability of nitric oxide through the formation of a novel nitrosothiol: implications for cardiovascular function and human disease. Nitric Oxide-Biol Chem 2006;14:A40.
[13] Fukuto J, Collins M. Interactive endogenous small molecule (gaseous) signaling: implications for teratogenesis. Curr Pharm Des 2007;13:2952–2978.
[14] Muzaffar S, Shukla N, Bond M, Newby AC, Angelini GD, Sparatore A, Soldato PD, Jeremy JY. Exogenous hydrogen sulfide inhibits superoxide formation, NOX-1 expression and Rac 1 activity in human vascular smooth muscle cells. J Vasc Res 2008;45:521–528.
[15] Kwak W, Kwon G, Jin I, Kuriyama H, Sohn H. Involvement of oxidative stress in the regulation of H_2S production during ultradian metabolic oscillation of Saccharomyces cerevisiae. FEMS Microbiol Lett 2003;219:99–104.
[16] Kimura Y, Kimura H. Hydrogen sulfide protects neurons from oxidative stress. FASEB J 2004;18:1165–1167.
[17] Hoffmann MR. Kinetics and mechanism of oxidation of hydrogen sulfide by hydrogen peroxide in acidic solution. Environ Sci Technol 1977;11:61–66.
[18] Cadena F, Peters R. Evaluation of chemical oxidizers for hydrogen sulfide control. J Water Poll Control Fed 1988;60:1259–1263.
[19] Yonezawa D, Sekiguchi F, Miyamotoa M, Taniguchi E, Honjo M, Masuko T, Nishikawa H, Kawabata A. A protective role of hydrogen sulfide against oxidative stress in rat gastric mucosal epithelium. Toxicology 2007;241:11–18.
[20] Chang L, Geng B, Yu F, Zhao J, Jiang H, Du J, Tang C. Hydrogen sulfide inhibits myocardial injury induced by homocysteine in rats. Amino Acids 2008;34:573–585.
[21] Lu M, Hu L, Hu G, Bian J. Hydrogen sulfide protects astrocytes against H_2O_2-induced neural injury via enhancing glutamate uptake. Free Radic Biol Med 2008;45:1705–1713.
[22] Devai I, Delaune R. Effectiveness of selected chemicals for controlling emission of malodorous sulfur gases in sewage sludge. Environ Technol 2002;23:319–329.
[23] Bartberger M, Olson L, Houk K. Mechanisms of peroxynitrite oxidations and rearrangements: the theoretical perspective. Chem Res Toxicol 1998;11:710–711.
[24] Whiteman M, Armstrong JS, Chu SH, Jia-Ling S, Wong B-S, Cheung NS, Halliwell B, Moore PK. The novel neuromodulator hydrogen sulfide: an endogenous peroxynitrite 'scavenger'? J Neurochem 2004;90:765–768.
[25] Dahm C, Moore K, Murphy M. Persistent S-nitrosation of complex I and other mitochondrial membrane proteins by S-nitrosothiols but not nitric oxide or peroxynitrite—implications for the interaction of nitric oxide with mitochondria. J Biol Chem 2006;281:10056–10065.
[26] Lobachev V, Rudakov E. The chemistry of peroxynitrite. Reaction mechanisms and kinetics. Uspekhi Khimii 2006;75:422–444.
[27] Whiteman M, Cheung N, Zhu Y, Chu S, Siau J, Wong B, Armstrong JS, Moore PK. Hydrogen sulphide: a novel inhibitor of hypochlorous acid-mediated oxidative damage in the brain? Biochem Biophys Res Commun 2005;326: 794–798.
[28] Laggner H, Muellner M, Schreier S, Sturm B, Hermann M, Exner M, Gmeiner BM, Kapiotis S. Hydrogen sulphide: a novel physiological inhibitor of LDL atherogenic modification by HOCl. Free Radic Res 2007;41:741–747.
[29] Chen KY, Morris JC. Oxidation of sulfide by O_2. Catalysis and inhibition. ASCE J Sanit Eng Div 1972;98:215–227.
[30] Tapley D, Buettner G, Shick J. Free radicals and chemiluminescence as products of the spontaneous oxidation of sulfide in seawater, and their biological implications. Biol Bull 1999;196:52–56.
[31] Dombkowski R, Russell M, Olson K. Hydrogen sulfide as an endogenous regulator of vascular smooth muscle tone in trout. Am J Physiol Regul Integr Comp Physiol 2004;286:R678–R685.
[32] Lide DR. CRC handbook of chemistry and physics.: CRC Press; 2005.
[33] Medvedeva ML, Gorelik AA. Dangers from improper use of aluminum tank cars. Chem Pet Eng 2007;43:695–698.
[34] Re R, Pellegrini N, Proteggente A, Pannala A, Yang M, Rice-Evans C. Antioxidant activity applying an improved ABTS radical cation decolorization assay. Free Radic Biol Med 1999;26:1231–1237.
[35] Staško A, Brezová V, Biskupič S, Mišík V. The potential pitfalls of using 1,1-diphenyl-2-picrylhydrazyl to characterize antioxidants in mixed water solvents. Free Radic Res 2007;41:379–390.
[36] Duling DR. Simulation of multiple isotropic spin-trap EPR-spectra. J Magn Reson B 1994;104:105–110.
[37] Hautala RR, Schore NE, Turro NJ. A novel fluorescent probe. Use of time-correlated fluorescence to explore the properties of micelle-forming detergent. J Am Chem Soc 1973;95:5508–5514.
[38] Bilski P, Chignell CF, Szychlinski J, Borkowski A, Oleksy E, Reszka K. Photooxidation of organic and inorganic substrates during UV photolysis of nitrite anion in aqueous solution. J Am Chem Soc 1992;114:549–556.
[39] Huvaere K, Andersen M, Storme M, Van Bocxlaer J, Skibsted L, De Keukeleire D. Flavin-induced photodecomposition of sulfur-containing amino acids is decisive in the formation of beer lightstruck flavor. Photochem Photobiol Sci 2006;5: 961–969.
[40] Lykakis I, Ferreri C, Chatgilialoglu C. The sulfhydryl radical ($HS^{\bullet}/S^{\bullet -}$): a contender for the isomerization of double bonds in membrane lipids. Angew Chem Int Ed 2007;46:1914–1916.
[41] Halliwell B, Gutteridge JMC. Free radicals in biology and medicine. Oxford: Oxford University Press; 1999.
[42] Makarov S, Mundoma C, Svarovsky S, Shi X, Gannett P, Simoyi R. Reactive oxygen species in the aerobic decomposition of sodium hydroxymethanesulfinate. Arch Biochem Biophys 1999;367:289–296.
[43] Rehorek D, Dubose C, Janzen E. On the spin trapping of sulfur-dioxide anion-radicals ($SO_2^{\bullet -}$) by nitrones. J Prakt Chem 1991;333:321–325.
[44] Covello PS, Thompson JE. Spin trapping evidence for formation of the sulfite radical anion during chloroplast-mediated oxidation of bisulfite ion. BBA General Subjects 1985;843:150–154.
[45] Chen C, Ren X, Lu D, Zhang Y. Study of photoreaction in aqueous dispersions of zinc-oxide containing inorganic salts. Chin Sci Bull 1991;36:1081–1085.
[46] Brezová V, Staško A, Biskupič S. Radical intermediates in the photochemical decomposition of p-toluenesulphonate (a kinetic spin-trapping study). J Photochem Photobiol A 1993;71:229–235.
[47] Jiang J, Liu KJ, Shi X, Swartz HM. Detection of short-lived free radicals by low-frequency electron paramagnetic resonance spin trapping in whole living animals. Arch Biochem Biophys 1995;319:570–573.

[48] Reed GA, Curtis JF, Mottley C. Epoxidation of (±)-7,8-dihydroxy-7,8-dihydrobenzo[*a*]pyrene during (bi)sulfite autoxidation: activation of a procarcinogen by a cocarcinogen. Proc Natl Acad Sci USA 1986;83:7499–7502.

[49] Mottley C, Connor H, Mason R. [^{17}O]oxygen hyperfine-structure for the hydroxyl and superoxide radical adducts of the spin traps DMPO, PBN and 4-POBN. Biochem Biophys Res Commun 1986;141:622–628.

[50] Moreno R, Alipazaga M, Gomes O, Linares E, Medeiros M, Coichev N. DNA damage and 2′-deoxyguanosine oxidation induced by S(IV) autoxidation catalyzed by copper(II) tetraglycine complexes: synergistic effect of a second metal ion. J Inorg Biochem 2007;101:866–875.

[51] Ilan Y, Rabani J. On some fundamental reactions in radiation chemistry: nanosecond pulse radiolysis. Int J Radiat Phys Chem 1976;8:609–611.

[52] Bielski B, Cabelli D, Arudi R, Ross A. Reactivity of HO_2/O_2^- radicals in aqueous-solution. J Phys Chem Ref Data 1985;14:1041–1100.

[53] Weinstein J, Bielski BHJ. Kinetics of the interaction of HO_2 and O_2^- radicals with hydrogen peroxide. The Haber-Weiss reaction. J Am Chem Soc 1979;101:58–62.

[54] Das T, Huie R, Neta P, Padmaja S. Reduction potential of the sulfhydryl radical: pulse radiolysis and laser flash photolysis studies of the formation and reactions of $^{\bullet}SH$ and $HSSH^{\bullet -}$ in aqueous solutions. J Phys Chem A 1999;103:5221–5226.

[55] Mills G, Schmidt KH, Matheson MS, Meisel D. Thermal and photochemical reactions of sulfhydryl radicals. Implications for colloid photocorrosion. J Phys Chem 1987;91:1590–1596.

[56] Creutz C, Sutin N. Kinetics of the reactions of sodium dithionite with dioxygen and hydrogen peroxide. Inorg Chem 1974;13:2041–2043.

[57] Report OECD SIDS. Sodium dithionite 7775-14-6. 2004. Available online at: http://www.inchem.org/documents/sids/sids/7775146.pdf,

[58] Huie RE, Neta P. Rate constants for some oxidations of S(IV) by radicals in aqueous solutions. Atmos Environ (1967) 1987;21:1743–1747.

[59] Huie RE, Neta P. Chemical behavior of SO_3^- and SO_5^- radicals in aqueous solutions. J Phys Chem 1984;88: 5665–5669.

[60] Huie RE, Clifton CL, Altstein N. A pulse radiolysis and flash photolysis study of the radicals SO_2^-, SO_3^-, SO_4^- and SO_5^-. Radiat Phys Chem 1989;33:361–370.

[61] Yermakov AN, Zhitomirsky BM, Poskrebyshev GA, Stoliarov SI. Kinetic study of SO_5^- and HO_2 radicals reactivity in aqueous phase bisulfite oxidation. J Phys Chem 1995;99:3120–3127.

[62] Goldstein S, Samuni A, Merenyi G. Kinetics of the reaction between nitroxide and thiyl radicals: nitroxides as antioxidants in the presence of thiols. J Phys Chem A 2008;112:8600–8605.

[63] Dabestani R, Hall R, Sik R, Chignell C. Spectroscopic studies of cutaneous photosensitizing agents—XV. Anthralin and its oxidation-product 1,8-dihydroxyanthraquinone. Photochem Photobiol 1990;52:961–971.

[64] Harbour JR, Hair ML. Detection of superoxide ions in nonaqueous media. Generation by photolysis of pigment dispersions. J Phys Chem 1978;82:1397–1399.

[65] Brezová V, Gabčová S, Dvoranová D, Staško A. Reactive oxygen species produced upon photoexcitation of sunscreens containing titanium dioxide (an EPR study). J Photochem Photobiol B 2005;79:121–134.

[66] Noda H, Oikawa K, Ohya-Nishiguchi H, Kamada H. Detection of superoxide ions from photoexcited semiconductors in non-aqueous solvents using the ESR spin-trapping technique. Bull Chem Soc Jpn 1993;66:3542–3547.

[67] Pieta P, Petr A, Kutner W, Dunsch L. *In situ* ESR spectroscopic evidence of the spin-trapped superoxide radical, $O_2^{\bullet -}$, electrochemically generated in dmso at room temperature. Electrochim Acta 2008;53:3412–3415.

[68] Lunenok-Burmakina VA, Gerasenkova AN. Mechanism of the oxidation of inorganic sulphur compounds by hydrogen peroxide. Russ J Inorg Chem 1964;9:149–152.

[69] Qiao X, Chen S, Tan L, Zheng H, Ding Y, Ping Z. Investigation of formation of superoxide anion radical in DMSO by ESR: Part 1. Influence of Fe^{2+} and Cu^{2+}. Magn Reson Chem 2001;39:207–211.

[70] Vasiltsov AM, Trofimov BA, Amosova SV, Voronov VK. Divinyl sulfide. Communication 9. Kinetics and mechanism of reaction of phenylacetylene with sodium hydrosulfide in aqueous dimethyl sulfoxide. Russ Chem Bull 1982;31: 2155–2160.

[71] Dalal N, Shi X. On the formation of oxygenated radicals by fredericamycin A and implications to its anticancer activity: An ESR investigation. Biochemistry 1989;28:748–750.

[72] Bors W, Stettmaier K. Determination of rate constants of the spin trap 3,5-dibromo-4 nitrosobenzenesulfonic acid with various radicals by pulse radiolysis and competition kinetics. J Chem Soc Perkin Trans 2 1992;:1509–1512.

[73] Stolze K, Mason RP. Spin trapping artifacts in DMSO. Biochem Biophys Res Commun 1987;143:941–946.

[74] Davies C, Nielsen B, Timmins G, Hamilton L, Brooker A, Guo R, Symons M, Winyard P. Characterization of the radical product formed from the reaction of nitric oxide with the spin trap 3,5-dibromo-4-nitrosobenzene sulfonate. Nitric Oxide 2001;5:116–127.

[75] Guo R, Davies C, Nielsen B, Hamilton L, Symons M, Winyard P. Reaction of the spin trap 3,5-dibromo-4-nitrosobenzene sulfonate with human biofluids. Biochim Biophys Acta Gen Subj 2002;1572:133–142.

[76] Geng B, Chang L, Pan C, Qi Y, Zhao J, Pang Y, Du J, Tanga C. Endogenous hydrogen sulfide regulation of myocardial injury induced by isoproterenol. Biochem Biophys Res Commun 2004;318:756–763.

[77] Fu Z, Liu X, Geng B, Fang L, Tang C. Hydrogen sulfide protects rat lung from ischemia–reperfusion injury. Life Sci 2008;82:1196–1202.

[78] Jha S, Calvert JW, Duranski MR, Ramachandran A, Lefer DJ. Hydrogen sulfide attenuates hepatic ischemia-reperfusion injury: role of antioxidant and antiapoptotic signaling. Am J Physiol Heart Circ Physiol 2008;295:H801–H806.

[79] Yan SK, Chang T, Wang H, Wu L, Wang R, Meng QH. Effects of hydrogen sulfide on homocysteine-induced oxidative stress in vascular smooth muscle cells. Biochem Biophys Res Commun 2006;351:485–491.

[80] Tyagi N, Moshal KS, Sen U, Vacek TP, Kumar M, Hughes WM Jr, Kundu S, Tyagi SC. H_2S protects against methionine-induced oxidative stress in brain endothelial cells. Antioxid Redox Signal 2009;11:25–33.

[81] Jeney V, Komódi E, Nagy E, Zarjou A, Vercellotti GM, Eaton JW, Balla G, Balla J. Supression of hemin-mediated oxidation of low-density lipoprotein and subsequent endothelial reactions by hydrogen sulfide (H_2S). Free Radic Biol Med 2009;46:616–623.

[82] Shi YX, Chen Y, Zhu YZ, Huang GY, Moore PK, Huang SH, Yao T, Zhu YC. Chronic sodium hydrosulfide treatment decreases medial thickening of intramyocardial coronary arterioles, interstitial fibrosis, and ROS production in spontaneously hypertensive rats. Am J Physiol Heart Circ Physiol 2007;293:H2093–H2100.

This paper was first published online on iFirst on 1 June 2009.